

This article was downloaded by:

On: 26 January 2011

Access details: *Access Details: Free Access*

Publisher *Taylor & Francis*

Informa Ltd Registered in England and Wales Registered Number: 1072954 Registered office: Mortimer House, 37-41 Mortimer Street, London W1T 3JH, UK



## Liquid Crystals

Publication details, including instructions for authors and subscription information:

<http://www.informaworld.com/smpp/title~content=t713926090>

### Molecular dynamics study of the ferroelectric liquid crystal CI IPNOC by proton spin-lattice relaxation

A. Ferraz<sup>a</sup>; J. L. Figueirinhas<sup>a</sup>; P. J. Sebastião<sup>a</sup>; A. C. Ribeiro<sup>a</sup>; H. T. Nguyen<sup>b</sup>; F. Noack<sup>c</sup>

<sup>a</sup> Centro de Física da Matéria Condensada (INIC), Lisboa Codex, Portugal <sup>b</sup> Centre de Recherche Paul Pascal Domain Universitaire, Talence, France <sup>c</sup> Physikalisches Institut der Universität Stuttgart, Stuttgart, Germany

**To cite this Article** Ferraz, A. , Figueirinhas, J. L. , Sebastião, P. J. , Ribeiro, A. C. , Nguyen, H. T. and Noack, F.(1993) 'Molecular dynamics study of the ferroelectric liquid crystal CI IPNOC by proton spin-lattice relaxation', *Liquid Crystals*, 14: 2, 415 – 426

**To link to this Article:** DOI: 10.1080/02678299308027656

**URL:** <http://dx.doi.org/10.1080/02678299308027656>

PLEASE SCROLL DOWN FOR ARTICLE

Full terms and conditions of use: <http://www.informaworld.com/terms-and-conditions-of-access.pdf>

This article may be used for research, teaching and private study purposes. Any substantial or systematic reproduction, re-distribution, re-selling, loan or sub-licensing, systematic supply or distribution in any form to anyone is expressly forbidden.

The publisher does not give any warranty express or implied or make any representation that the contents will be complete or accurate or up to date. The accuracy of any instructions, formulae and drug doses should be independently verified with primary sources. The publisher shall not be liable for any loss, actions, claims, proceedings, demand or costs or damages whatsoever or howsoever caused arising directly or indirectly in connection with or arising out of the use of this material.

## Molecular dynamics study of the ferroelectric liquid crystal CI IPNOC by proton spin-lattice relaxation

by A. FERRAZ, J. L. FIGUEIRINHAS\*, P. J. SEBASTIÃO,  
and A. C. RIBEIRO

Centro de Física da Matéria Condensada (INIC), Av. Prof. Gama Pinto, 2,  
1699 Lisboa Codex, Portugal

and H. T. NGUYEN

Centre de Recherche Paul Pascal Domain Universitaire, 33405 Talence, France

and F. NOACK

Physikalisches Institut der Universität Stuttgart, 7000 Stuttgart-80, Germany

Proton spin-lattice relaxation studies were carried out in the  $S_A$  and  $S_C^*$  phases of the liquid crystal CI IPNOC using both conventional and fast field cycling NMR techniques.  $T_1$  dispersion curves were obtained at two different temperatures for each mesophase covering frequencies from  $10^2$  to  $3 \times 10^8$  Hz. In both mesophases the  $T_1$  data can be described assuming the presence of three different relaxation mechanisms, namely local molecular rotations, molecular self-diffusion and collective motions. The self-diffusion constant  $D_{\perp}$  was evaluated for several temperatures and the activation energy associated with the diffusion process was obtained. The expected contribution of the soft-mode for the spin-lattice relaxation could not be separated from the contribution of other collective motions. The correlation times associated with the rotations around the molecular long axis and with the fluctuations of this axis were evaluated for both the  $S_A$  and the  $S_C^*$  phases.

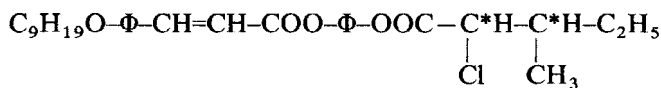
### 1. Introduction

The technological potential of ferroelectric liquid crystals has recently produced a growing interest in these materials. A great number of both theoretical [1–7] and experimental publications [7–16] on these systems is becoming available in the literature. The behaviour of the main physical quantities, such as molecular tilt and spontaneous polarization, can in general be explained by existing theories based either on the Landau–de Gennes free energy expansion [2, 4, 5, 7] or on statistical models [3, 6]. The dynamics of these systems has also been worked out [1, 2, 5, 9] and numerous experimental studies have obtained the dispersion curves of the dielectric permittivity which allow identification of the contributions of both the Goldstone- and soft-modes [5, 7, 9, 11] in the  $S_C^*$  phase. Proton spin-lattice relaxation can complete the view of ferroelectric liquid crystal systems since it is dependent both on the rapid local molecular rotations thought to play a role in the existence of the in-plane spontaneous polarization and the collective molecular motions associated with layer undulations and the soft-mode. The Goldstone-mode, also present in the  $S_C^*$  phase, has too low a characteristic frequency to be detectable by proton NMR relaxation. The correlation time associated with rotations around the molecular long axis may be evaluated and

\* Author for correspondence.

this can contribute to clarifying the existing controversy regarding the possible existence of a slowing down of this rotation at the  $S_A$ - $S_C^*$  transition, as claimed by Lalanne *et al.* [12].

Following proton NMR relaxation studies performed on the ferroelectric liquid crystal DOBAMBC [8, 13], we present here new relaxation results obtained with the compound Cl IPNOC (2-(*S*),3(*S*)-2-chloro-3-methyl pentanoyloxyphenyl 4-nonyloxy-cinnamate), which shows the following phase transitions:



C 68°C  $S_C^*$  78°C  $S_A$  95°C N\* 97°C I.

## 2. Experimental

The synthesis of the liquid crystal material Cl IPNOC is described in [17]. The NMR samples were prepared by sealing a few hundred milligrams in a NMR glass tube under moderate vacuum ( $10^{-4}$  T). The low frequency range ( $\omega/2\pi = 100$  Hz to 4 MHz) of the  $T_1$  dispersion data was obtained using a field cycling spectrometer [18] with a polarization and detection field of 0.215 T and a switching time of 2–3 ms. The high frequency range (4 MHz to 300 MHz) of the  $T_1$  dispersion data, as well as the  $T_1$  angular dependence measured at 60 MHz were obtained in conventional NMR pulsed spectrometers (Bruker SXP 4-100 and MSL 300) using the inversion recovery sequence with phase cycling to eliminate the DC bias. The measurements were carried out after increasing the temperature to the isotropic phase followed by slow cooling to the desired sample temperature in the presence of the magnetic field.

## 3. Theory

The proton spin-lattice relaxation in the less ordered liquid crystalline phases like the nematic and the in-plane liquid phases,  $S_A$  and  $S_C$ , is generally accepted as depending on three different relaxation mechanisms, namely order director fluctuations (ODF), molecular self-diffusion (SD) and local molecular rotations (ROT) [19–21]. The last two contributions are also the relevant relaxation mechanisms in isotropic fluids [22].

In a full analysis of the relaxation rate, cross terms between the contributions of these three mechanisms should be taken into account. While an approach which takes into account, simultaneously, order director fluctuations and local molecular rotations was put forward by Freed [23] for the nematic phase, no general theory is available which allows the calculation of these cross terms for the mesophases under discussion. The contribution of cross terms to the relaxation rate has generally been neglected in the literature due to the large difference in time scales for the three relaxation mechanisms described above. A similar approach is followed here.

Order director fluctuations with a dispersion law for  $T_1$  proportional to  $\omega^{1/2}$  were observed as the predominant relaxation mechanism in nematics for frequencies below a few MHz [18, 24]. The same type of frequency dependence was also predicted for the ODF mechanism in  $S_A$  phases [25]. However,  $T_1$  becomes proportional to  $\omega$  when layer undulations are the predominant collective motions present in these kinds of mesophases [19]. Usually, order director fluctuations become an important relaxation mechanism for the  $S_A$  and  $S_C$  phases only in the kHz range [24, 26].

The presence of anharmonic effects in the hydrodynamics of  $S_A$  and  $S_C$  phases introduces singularities in the wave vector ( $\mathbf{q}$ ) and frequency ( $\omega$ ) dependencies of the viscosities and elastic constants. Even though these are logarithmic for the elastic constants [27], special care has to be taken when calculating effective viscosities and elastic constants from the fitting parameters, since the theoretical expressions for the relaxation rate by order director fluctuations do not take into account these singularities.

Spin-lattice relaxation produced by molecular self-diffusion in isotropic liquids was first treated in a simplified way in Abragam's book [22]. An improvement was introduced later by Torrey [28] with his theory based on a random flight approach to the diffusion process. While Torrey's theory has also been used for anisotropic fluids such as liquid crystals, its validity in the low frequency region is questionable and it does not explain the experimentally detected angular dependence of  $T_1$ . A development of Torrey's theory proposed later [29] for anisotropic fluids seems much more appropriate and will be considered here.

Local molecular rotations and conformational changes of the aliphatic chains become, in these phases, a predominant relaxation mechanism in the high frequency region, typically above 30 MHz. Though the initial one correlation time model introduced for this mechanism [22] is acceptable for isotropic fluids, it becomes less suitable for more ordered phases such as those considered here. In particular, it cannot predict the  $T_1$  angular dependence observed experimentally for these phases. More elaborate models for the relaxation rate due to local molecular rotations were proposed in the literature. Basically two diffusion coefficients [30] or alternatively two correlation times [21, 31] are used to characterize the local molecular motions. One correlation time is associated with rotations around the molecular long axis and the other characterizes the polar fluctuations of this axis. Another model where three correlation times are used to describe the local molecular motions was also put forward [32]. This model considers rotations around the molecular long axis and fluctuations of this axis in a mean field potential of the Maier-Saupe type without coupling between the two processes. One correlation time,  $\tau_{\parallel}$ , characterizes the rotation around the molecular long axis and the other two correlation times,  $\tau_{\perp}$  and  $\tau_{\parallel}$ , characterize the motion of the molecular long axis in the laboratory frame.  $\tau_{\perp}$  is the correlation time associated with polar motions and  $\tau_{\parallel}$  the correlation time associated with azimuthal motions.

Fits of the experimental results with both this model [32] (referred to as model I) and the other model mentioned previously [21] (referred to as model II) were obtained and the results compared.

In both cases the overall spin-lattice relaxation rate  $1/T_1$  will be given by

$$\frac{1}{T_1} = \frac{1}{T_{1(\text{ODF})}} + \frac{1}{T_{1(\text{SD})}} + \frac{1}{T_{1(\text{ROT})}} \quad (1)$$

where possible cross terms between the different mechanisms are neglected.

As will be pointed out in the data analysis, the contribution of the collective motions to the spin lattice relaxation is better described in both mesophases by a  $T_1$  frequency dependence of the type  $T_1 \propto \omega^1$  than by  $T_1 \propto \omega^{1/2}$ . In the case of a fully oriented sample with the director parallel to the magnetic field the contribution from the mechanism of order director fluctuations is [19]

$$\frac{1}{T_{1(\text{ODF})}} = \frac{9}{8} \gamma^4 \hbar^2 J_1(\omega) = \frac{9}{8} \gamma^4 \hbar^2 \frac{A}{\omega} \left[ \arctg\left(\frac{\omega_1}{\omega}\right) - \arctg\left(\frac{\omega_0}{\omega}\right) \right], \quad (2)$$

where  $\gamma$  is the gyromagnetic ratio for protons,  $\hbar$  is Planck's constant divided by  $2\pi$ ,  $J_1(\omega)$  is a spectral density and  $A$  is an adjustable parameter which depends on the temperature, the nematic order parameter  $S$  and material physical constants.  $\omega_0$  and  $\omega_1$  are the low and high cut-off frequencies of the ODF modes, respectively, depending on the effective viscosity, splay elastic constant and smallest and largest wave vectors present in the system.

The contribution from the molecular self-diffusion is given by [29]

$$\frac{1}{T_{1(\text{SD})}} = \frac{9}{8} \gamma^4 \hbar^2 (J_1(\omega) + J_2(2\omega))_{(\text{SD})} = \frac{9}{8} \gamma^4 \hbar^2 \frac{n}{d^3} \tau_{d\perp} R \left( \omega \tau_{d\perp}; \frac{\langle r_{\perp}^2 \rangle}{d^2}; \frac{D_{\parallel}}{D_{\perp}}; \frac{l}{d}; \beta \right), \quad (3)$$

where  $J_1(\omega)$  and  $J_2(\omega)$  are spectral densities,  $\langle r_{\perp}^2 \rangle = 4D_{\perp} \tau_{d\perp}$  and  $\beta$  is the angle between the director and the magnetic field. For simplicity, the following values were used [33]

$$\frac{\langle r_{\perp}^2 \rangle}{d^2} = 1, \quad \frac{D_{\parallel}}{D_{\perp}} = 1.$$

The value  $l/d$  is approximately the length of the molecule over its diameter and is around 7 in our case.  $n$  is the spin density and was taken as  $5 \times 10^{28} \text{ m}^{-3}$ . The adjustable parameters are  $\tau_{d\perp}$  and  $d$ , with  $d$  expected to be around  $5 \times 10^{-10} \text{ m}$ .

The contribution from local molecular rotations according to model I [32] is given by

$$\begin{aligned} \frac{1}{T_{1(\text{ROT})}} &= \frac{9}{8} \gamma^4 \hbar^2 (J_1(\omega) + J_2(2\omega))_{(\text{ROT})} \\ &= \frac{9}{8} \gamma^4 \hbar^2 \left( \frac{2}{9} \sum_{l=-2}^{l=2} C_{1l} A_l \sum_{j=1}^n a_{j1l} \frac{\tau_{j1l}}{1 + \omega^2 \tau_{j1l}^2} \right. \\ &\quad \left. + \frac{8}{9} \sum_{l=-2}^{l=2} C_{2l} A_l \sum_{j=1}^n a_{j2l} \frac{\tau_{j2l}}{1 + 4\omega^2 \tau_{j2l}^2} \right), \end{aligned} \quad (4)$$

where  $C_{ij}$ ,  $a_{jkl}$  and  $b_{ijk}$  were obtained from [32] for specific values of the nematic order parameter  $S$ . The quantities  $A_l$  and  $\tau_{ijk}$  are

$$A_l = C \frac{1}{N_0} \sum_{j>i}^{N_0} \frac{1}{r_{ij}^6} \left\{ \begin{array}{ll} \frac{3}{2} (1 - 3 \cos^2 \alpha_{ij})^2, & (l=0) \\ \frac{9}{4} \sin^2 2\alpha_{ij}, & (l=\pm 1) \\ \frac{9}{4} \sin^4 \alpha_{ij}, & (l=\pm 2) \end{array} \right\}; \quad \tau_{ijk}^{-1} = \frac{1}{b_{ijk} \tau_k} + K_k,$$

with

$$K_k = \left\{ \begin{array}{ll} 0 & (k=0) \\ 1/\tau_y & (k=1) \\ (3p+1)/\tau_y & (k=2) \end{array} \right\}; \quad \tau_k = \left\{ \begin{array}{ll} \tau_{\perp} & (k=0) \\ \left( \frac{5}{6} \tau_{\perp}^{-1} + \frac{1}{6} \tau_{\parallel}^{-1} \right)^{-1} & (k=1) \\ \left( \frac{2}{6} \tau_{\perp}^{-1} + \frac{4}{6} \tau_{\parallel}^{-1} \right)^{-1} & (k=2) \end{array} \right\}. \quad (5)$$

$N_0$  is the number of protons per molecule,  $r_{ij}$  is the inter-proton distance and  $\alpha_{ij}$  is the angle between the molecular long axis and the inter-proton vector. The  $A_i$  factors were calculated considering the molecule in the all-*trans*-conformation with  $C$  as an adjustable parameter to correct eventually the conformation's deviation from all-*trans*.

The adjustable parameters are

- (i)  $p$ , which is 1 for a small step rotation process and 0 for a strong collision type process;
- (ii)  $\tau_\gamma$ ,  $\tau_\perp$  and  $\tau_\parallel$ , as described above.

When the director is not parallel to the external magnetic field, the spectral densities  $J_i$  also become functions of the angle  $\beta$  between the magnetic field and the director  $\mathbf{n}$ . If a distribution of director orientations is present in the sample, as in the  $S_C^*$  phase, the spectral densities are given by

$$J_i(\omega, \Delta) = \int_0^{2\pi} \int_0^\pi J_i[\omega, \beta(\theta, \varphi, \Delta)] P(\theta) \sin \theta \, d\theta \, d\varphi$$

(6)

with

$$\beta(\theta, \varphi, \Delta) = \arccos(\sin \Delta \sin \theta \cos \varphi + \cos \Delta \cos \theta)$$

and

$$J_i(\omega, \beta) = \left\{ \begin{array}{ll} 1 - 3 \sin^2 \beta + \frac{9}{4} \sin^4 \beta & (i=0) \\ \frac{1}{4} (\sin^2 \beta - \sin^4 \beta) & (i=1) \\ \frac{1}{4} \sin^4 \beta & (i=2) \end{array} \right\} J_0(\omega)$$

$$+ \left\{ \begin{array}{ll} 18 (\sin^2 \beta - \sin^4 \beta) & (i=0) \\ 1 - \frac{5}{2} \sin^2 \beta + 2 \sin^4 \beta & (i=1) \\ 2(2 \sin^2 \beta - \sin^4 \beta) & (i=2) \end{array} \right\} J_1(\omega)$$

$$+ \left\{ \begin{array}{ll} \frac{9}{8} \sin^4 \beta & (i=0) \\ \frac{1}{8} (2 \sin^2 \beta - \sin^4 \beta) & (i=1) \\ 1 - \sin^2 \beta + \frac{1}{8} \sin^4 \beta & (i=2) \end{array} \right\} J_2(\omega). \quad (7)$$

$\Delta$  is the angle of rotation of the sample in the magnetic field or equivalently, the angle between the direction of the average director orientations ( $\Sigma \mathbf{n}_i = \mathbf{z}'$ ) and the magnetic field;  $\theta$  and  $\varphi$  are the angles, in spherical coordinates, of each director  $\mathbf{n}_i$  in the  $(x', y', z')$  frame, as shown in figure 1.  $P(\theta)$  is the director orientation distribution function, assuming a uniform distribution over  $\varphi$ . The factors between brackets are the usual factors for rotation of the spectral densities [34].

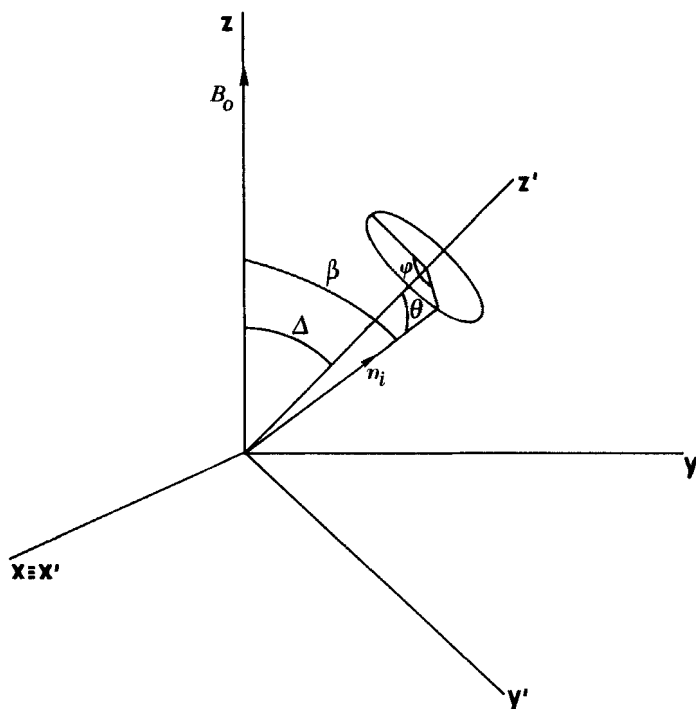


Figure 1. Coordinate systems used to model the rotation of the sample in the magnetic field. The notation is explained in the text.

#### 4. Data and analysis

The spin-lattice relaxation dispersion curves were obtained covering the frequency range ( $\omega/2\pi$ ) from  $10^2$  to  $3 \times 10^8$  Hz. The results for two temperatures in the  $S_A$  phase and two temperatures in the  $S_C^*$  phase are shown in figure 2. The angular dependence of  $T_1$  was also evaluated at 60 MHz for all the temperatures as shown in figure 3. In both mesophases, equation (1) was fitted to the experimental data by a non-linear least-squares optimization process.

##### 4.1. $S_A$ phase

For the analysed temperatures, the  $T_1$  dispersion profiles clearly show the presence of at least three dominant relaxation mechanisms with different characteristic correlation times. These mechanisms were identified as collective motions, molecular self-diffusion and local molecular rotations. The angular dependence of the proton spectra further indicates that the sample has a good degree of alignment in this phase, compatible with the strong  $T_1$  angular dependence experimentally obtained. To take these experimental observations into account, the spectral densities  $J_1(\omega, \Delta)$  and  $J_2(2\omega, \Delta)$  were calculated, using for the director orientation distribution function  $P(\theta)$  a gaussian law centred at zero and with a narrow width, below  $10^\circ$ . Both the predicted  $\omega^{-1/2}$  and  $\omega^{-1}$  frequency dependence laws for the contribution of the order director fluctuations to the relaxation rate were tested in the fits. The best results were obtained with the  $\omega^{-1}$  type law indicated above. Acceptable results with the  $\omega^{-1/2}$  law could only be obtained with unphysical cut-off frequencies. The fit for the  $T_1$  dispersion data using model I at  $90^\circ\text{C}$  is shown in figure 4, with the contributions from the different

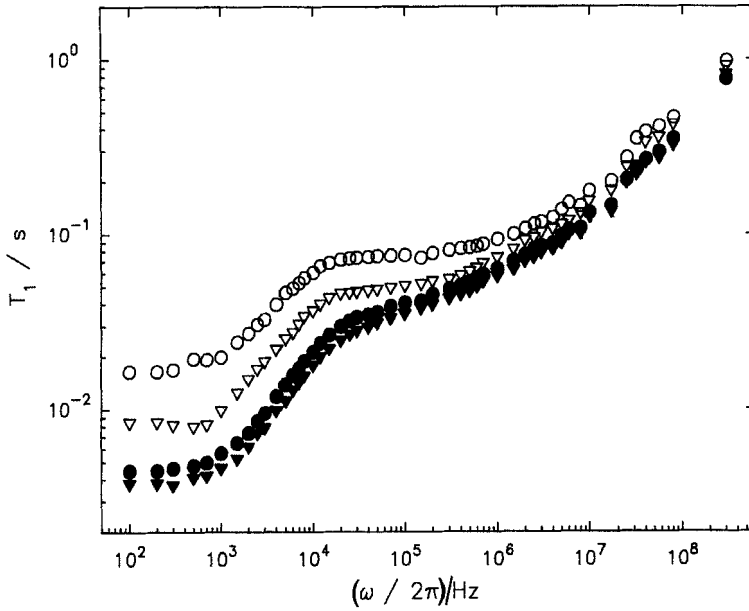


Figure 2. Frequency dependence of the spin-lattice relaxation time  $T_1$  for two temperatures in the  $S_A$  phase and two temperatures in the  $S_C^*$  phase.  $\circ$ ,  $T=90^\circ\text{C}$  ( $S_A$ );  $\nabla$ ,  $T=82^\circ\text{C}$  ( $S_A$ );  $\bullet$ ,  $T=74^\circ\text{C}$  ( $S_C^*$ );  $\blacktriangledown$ ,  $T=70^\circ\text{C}$  ( $S_C^*$ ).

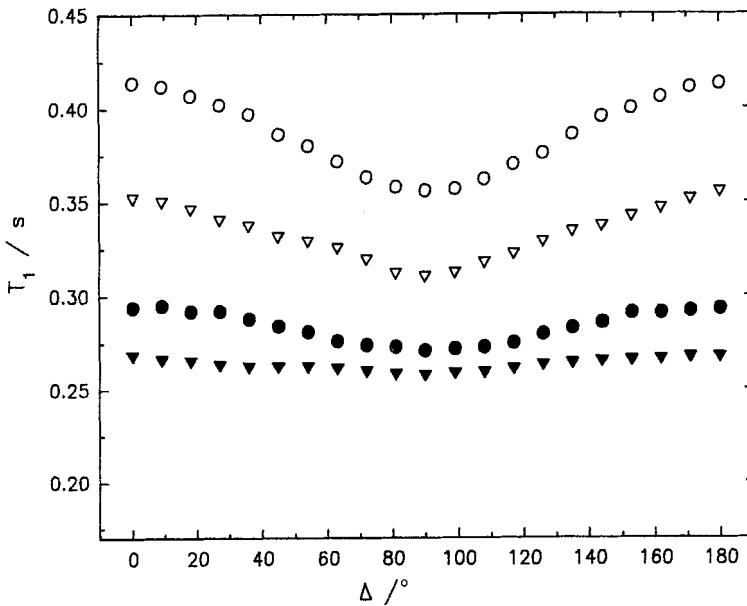


Figure 3. Angular dependence of the spin-lattice relaxation time  $T_1$  measured at  $\omega/2\pi=60$  MHz in the  $S_A$  and  $S_C^*$  phases for four different temperatures.  $\circ$ ,  $T=90^\circ\text{C}$  ( $S_A$ );  $\nabla$ ,  $T=82^\circ\text{C}$  ( $S_A$ );  $\bullet$ ,  $T=74^\circ\text{C}$  ( $S_C^*$ );  $\blacktriangledown$ ,  $T=70^\circ\text{C}$  ( $S_C^*$ ).



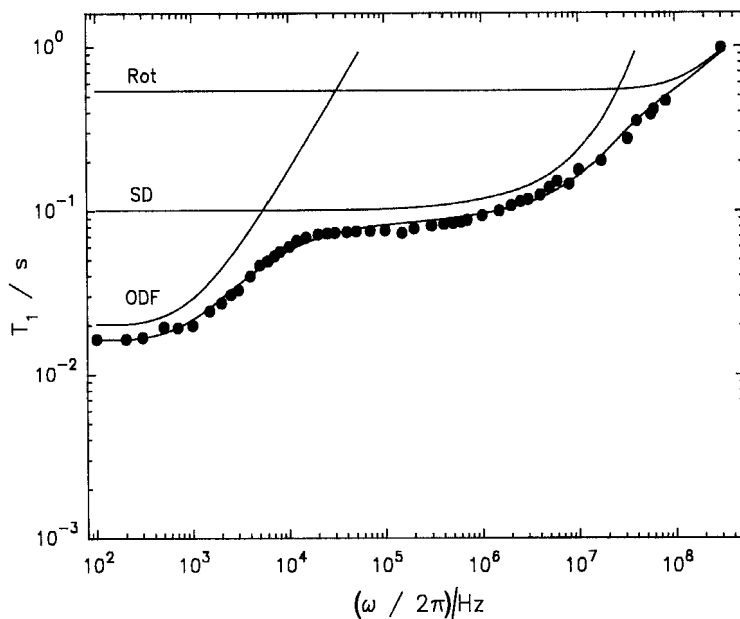


Figure 4. Fit of  $T_1$  (see equation (1)) to the experimental data as a function of  $\omega/2\pi$ , in the  $S_A$  phase at  $90^\circ\text{C}$ . The contributions of the different relaxation mechanisms are shown.

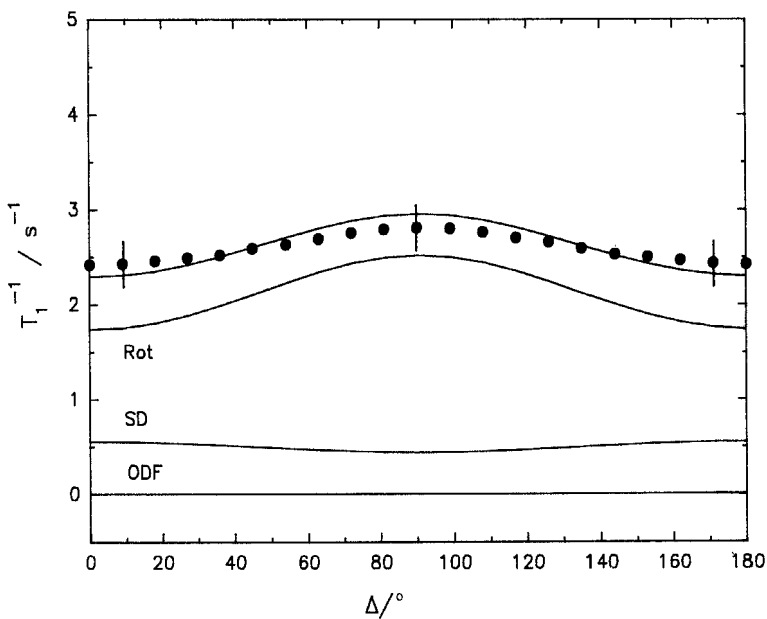


Figure 5. Fit of  $1/T_1$  (see equation (1)) to the experimental data, as a function of the angle  $\Delta$  at  $T=90^\circ\text{C}$ , in the  $S_A$  phase and for  $\omega/2\pi=60$  MHz. The contributions of the different relaxation mechanisms are shown.

relaxation mechanisms. A similar fit was obtained at 82°C. Model II produced similar quality fits and so they will not be shown. The fit for the  $T_1^{-1}$  angular dependence at 90°C for  $\omega/2\pi=60$  MHz, using model I, is shown in figure 5 along with the contributions from the different relaxation mechanisms. A similar fit was obtained at 82°C. The table presents the values of the fitted parameters. The fitting parameters characterizing the diffusion are  $d$  and  $\tau_{d\perp}$ . The value obtained for  $d$  at all temperatures is in the range generally accepted for the intermolecular distance within smectic layers. The values of the diffusion constant  $D_{\perp}$ , obtained from  $\tau_{d\perp}$ , are within the range expected for  $S_A$  phases [33]. The fitting parameters characterizing the rotation process are  $\tau_{\gamma}$ ,  $\tau_{\perp}$ ,  $\tau_{\parallel}$  and  $p$  for model I, and  $\tau_{\perp}$  and  $\tau_{\parallel}$  for model II.  $p$  is seen to be 0 at all temperatures, which indicates a strong collision type process for the molecular rotation around the molecular long axis. Only a rough estimate for the correlation time  $\tau_{\parallel}$  from model I can be obtained from the fits, since it experimentally involves a large uncertainty. If a comparison is drawn between  $\tau_{\perp}$  of the two models, and between  $\tau_{\gamma}$  of model I and  $\tau_{\parallel}$  of model II, which respectively should have a similar meaning, the agreement is far from good. This may indicate that  $\tau_{\perp}$  and  $\tau_{\parallel}$  from model II are contributed to simultaneously by both rotations around the molecular long axis and fluctuations of this axis, because these two mechanisms are treated in a simpler way than in model I.

#### 4.2. $S_C^*$ phase

As in the  $S_A$  phase, three relaxation mechanisms are seen to dominate the  $T_1$  dispersion data at all temperatures analysed, namely: collective motions (layer undulations), molecular self-diffusion and local molecular rotations. Surprisingly, as in

Model parameters obtained from the best fits of the experimental data to equation (1) at different temperatures in the  $S_A$  and  $S_C^*$  phases as described in the text. The results of the fitting parameters obtained with Models I and II for rotations are compared. The nematic order parameter  $S$  was estimated from the proton NMR spectra. The notation is explained in the text.

		$S_A$ phase		$S_C^*$ phase	
$T/^\circ\text{C}$		90	82	74	70
$S$		0.69	0.71	0.72	0.72
ODF Model	$A/10^{-7} \text{ \AA}^{-6}$	1.1	2.3	5.3	6.3
	$(\omega_0/2\pi)/\text{kHz}$	0.8	0.9	1.4	1.6
	$(\omega_1/2\pi)/\text{MHz}$	380	380	380	380
SD + ROT Model I	$d/10^{-10} \text{ m}$	4.6	4.6	4.6	4.6
	$\tau_d/10^{-9} \text{ s}$	4.4	5.2	5.8	6.4
	$D_{\perp}/10^{-11} \text{ m}^2 \text{ s}^{-1}$	1.22	1.03	0.92	0.84
	$p$	0.0	0.0	0.0	0.0
	$\tau_{\perp}/10^{-9} \text{ s}$	1.02	1.71	2.5	3.0
	$\tau_{\parallel}/10^{-9} \text{ s}$	$\approx 1$	$\approx 1$	$\approx 1$	$\approx 1$
SD + ROT Model II	$d/10^{-10} \text{ m}$	4.6	4.6	4.6	4.6
	$\tau_d/10^{-9} \text{ s}$	4.4	5.8	6.6	7.5
	$D_{\perp}/10^{-11} \text{ m}^2 \text{ s}^{-1}$	1.22	0.92	0.81	0.72
	$\tau_{\perp}/10^{-10} \text{ s}$	4.3	5.1	6.9	8.5
	$\tau_{\parallel}/10^{-10} \text{ s}$	1.7	2.4	2.6	2.7
	$\tau_{\gamma}/10^{-11} \text{ s}$	3.3	3.9	5.0	5.4

the  $S_A$  phase, the expected contribution of the soft-mode for the spin-lattice relaxation rate was not separable from the contribution of layer undulations. In this phase the angular dependence of the dipolar splitting shows a high degree of misalignment, in agreement with the weak  $T_1$  angular dependence detected experimentally. To take these experimental observations into account, the spectral densities  $J_1(\omega, \Delta)$  and  $J_2(2\omega, \Delta)$  were calculated using a distribution of sample domain orientations, in accordance with the observed angular dependent proton spectra. The director orientation distribution function  $P(\theta)$  was then approximated by a gaussian distribution peaked at zero and whose width was obtained from the proton spectra. As in the  $S_A$  phase, both the predicted  $\omega^{-1/2}$  and  $\omega^{-1}$  frequency dependence laws for the contribution of the order director fluctuations to the relaxation rate were tested in the fits. The best results were found with the  $\omega^{-1}$  type law indicated above. As in the  $S_A$  phase, acceptable results with the  $\omega^{-1/2}$  law could only be obtained with unphysical cut-off frequencies. The fit for the  $T_1$  dispersion data at  $74^\circ\text{C}$  using model I is shown in figure 6, with the contributions from the different relaxation mechanisms. A similar fit was obtained at  $70^\circ\text{C}$ . Model II produced fits of similar quality and so they will not be shown. The fit for the  $T_1^{-1}$  angular dependence at  $74^\circ\text{C}$  for  $\omega/2\pi = 60$  MHz, using model I, is shown in figure 7, along with the contributions from the different relaxation mechanisms. The table presents the values of the fitting parameters obtained from the data fitting optimization.

By analysing the temperature dependence of  $D_\perp$  for both the  $S_A$  and  $S_C^*$  phases, we see that it follows an Arrhenius-type law with an activation energy that is somewhat dependent upon the model considered for local molecular rotations; it is  $18 \text{ kJ mol}^{-1}$  with model I and  $26 \text{ kJ mol}^{-1}$  with model II. The temperature dependence of  $\tau_\perp$  from both models in both mesophases is also seen to obey an Arrhenius-type law with activation energies equal to  $52 \text{ kJ mol}^{-1}$  for model I and  $33 \text{ kJ mol}^{-1}$  for model II. The correlation times for the molecular rotations around the molecular long axis,  $\tau$ , if we

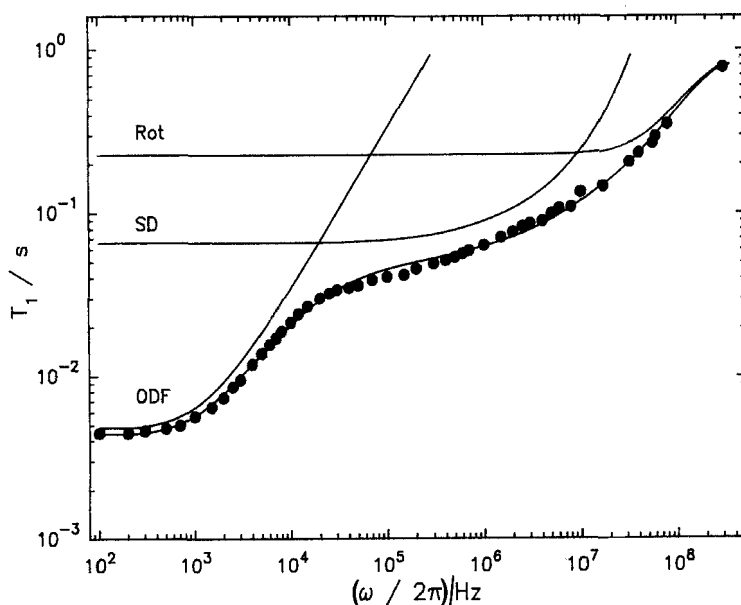


Figure 6. Fit of  $T_1$  (see equation (1)) to the experimental data, as a function of  $\omega/2\pi$ , in the  $S_C^*$  phase at  $74^\circ\text{C}$ . The contributions of the different relaxation mechanisms are shown.

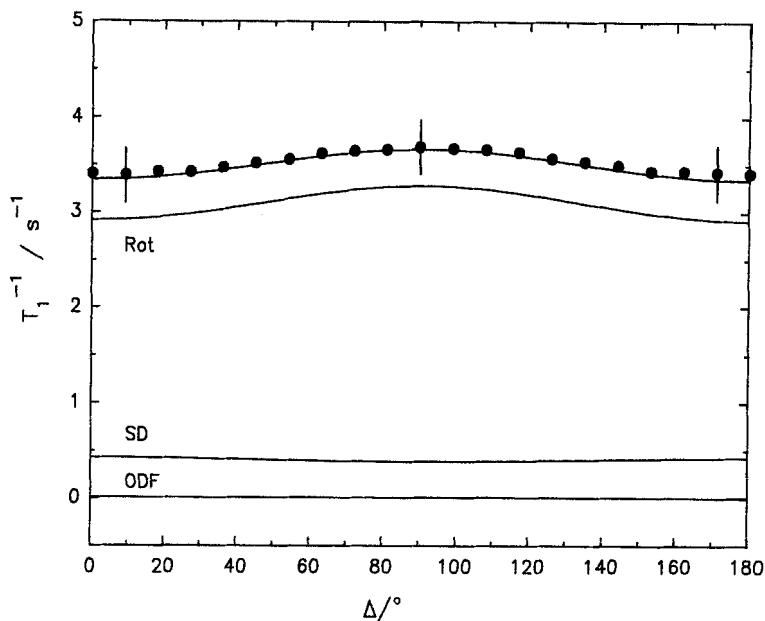


Figure 7. Fit of  $1/T_1$  (see equation (1)) to the experimental data, as a function of the angle  $\Delta$  at  $T = 74^\circ\text{C}$ , in the  $S_C^*$  phase and for  $\omega/2\pi = 60$  MHz. The contributions of the different relaxation mechanisms are shown.

consider model I and  $\tau_{\parallel}$  if we consider model II, seem to display a temperature evolution over the two mesophases in accordance with an Arrhenius-type law. The activation energies for  $\tau_{\gamma}$  and  $\tau_{\parallel}$  of model II are  $26 \text{ kJ mol}^{-1}$  and  $22 \text{ kJ mol}^{-1}$ , respectively. Comparing the results from the two models, model II gives a lower value for  $\tau_{\perp}/\tau_{\parallel}$  than expected from the structure of the mesophases, while model I gives a more reasonable value for the equivalent ratio  $\tau_{\perp}/\tau_{\gamma}$ . We believe that model I gives more realistic values for  $\tau_{\perp}$  and  $\tau_{\gamma}$ , but only an independent study using other experimental techniques could confirm this.

## 5. Conclusion

The proton spin-lattice relaxation data obtained for the  $S_C^*$  phase shows the presence of three relaxation mechanisms as known for  $S_A$  and achiral  $S_C$  phases. The possible contribution of the soft-mode for the proton spin-lattice relaxation could not be separated from the contribution of layer undulations. The values of the diffusion constants are in the range expected for  $S_A$  and  $S_C$  mesophases [33]. The correlation time associated with rotations around the molecular long axis increases on going from the  $S_A$  to the  $S_C^*$  phase, with a temperature dependence in accordance with an Arrhenius-type law. A slowing down of the molecular rotation around its long axis at the  $S_A$ - $S_C^*$  transition is only compatible with these data if followed by an increase in the molecular rate associated with this motion immediately below the  $S_A$ - $S_C^*$  transition.

We wish to thank ICTPOL for the use of the MSL-300 spectrometer. We acknowledge JNICT for financial support (Project STRDA/500/CEN).

## References

- [1] BLINC, R., 1975, *Phys. Stat. Sol.*, **70**, K29.
- [2] BLINC, R., and ZEKS, B., 1978, *Phys. Rev. A*, **18**, 740.
- [3] OSIPOV, M. A., and PIKIN, S. A., 1983, *Molec. Crystals liq. Crystals*, **103**, 57.
- [4] ZEKS, B., 1984, *Molec. Crystals liq. Crystals*, **114**, 259.
- [5] BLINC, R., FILIPIC, C., LEVSTIK, A., ZEKS, B., and CARLSSON, T., 1987, *Molec. Crystals liq. Crystals*, **151**, 1.
- [6] BERESNEV, L. A., BLINOV, L. M., OSIPOV, M. A., and PIKIN, S. A., 1988, *Molec. Crystals liq. Crystals A*, **158**, 3.
- [7] MUSEVIC, I., BLINC, R., ZEKS, B., FILIPIC, C., COPIC, M., SEPPEN, A., WYDER, P., and LEVANYUK, A., 1988, *Phys. Rev. Lett.*, **60**, 1530.
- [8] DONG, R. Y., and SANDEMAN, J., 1983, *J. Chem. Phys.*, **78**, 7, 4649; VIFAN, M., BLINC, R., and RUTAR, V., 1984, *Molec. Crystals liq. Crystals*, **114**, 271.
- [9] LEVSTIK, A., CARLSSON, T., FILIPIC, C., LEVSTIK, I., and ZEKS, B., 1987, *Phys. Rev. A*, **35**, 3527.
- [10] RIEKER, T. P., CLARK, N. A., SMITH, G. S., PARMER, D. S., SIROTA, E. B., and SAFINYA, C. R., 1987, *Phys. Rev. Lett.*, **59**, 2658.
- [11] BIRADAR, A. M., WRÖBEL, S., and HAASE, W., 1989, *Liq. Crystals*, **5**, 1227.
- [12] LALANNE, J. R., BUCHERT, J., DESTRADE, C., NGUYEN, H. T., and MARCEROU, J. P., 1989, *Phys. Rev. Lett.*, **62**, 3046; LALANNE, J. R., DESTRADE, C., NGUYEN, H. T., and MARCEROU, J. P., 1991, *Phys. Rev. A*, **44**, 6632.
- [13] BENDER, H., NOACK, F., VILFAN, M., and BLINC, R., 1989, *Liq. Crystals*, **5**, 1233.
- [14] BUKA, A., SIEMENSMEYER, K., and STEGEMEYER, H., 1989, *Liq. Crystals*, **6**, 701.
- [15] KREMER, F., VALLERIEU, U., KAPITZA, H., ZENTEL, R., and FISCHER, E. W., 1990, *Phys. Rev. A*, **42**, 3667.
- [16] GOUDA, F., SKARP, K., and LAGERWALL, S. T., 1991, *Ferroelectrics*, **113**, 165.
- [17] NGUYEN, H. T., SALENEUVE, C., and DESTRADE, C., 1988, *Ferroelectrics*, **85**, 823.
- [18] NOACK, F., 1986, *Prog. NMR Spectrosc.*, **18**, 171.
- [19] BLINC, R., LUZAR, M., VILFAN, M., and BURGAR, M., 1975, *J. chem. Phys.*, **63**, 3445.
- [20] BLINC, R., VILFAN, M., LUZAR, M., SELIGER, J., and ZAGAR, V., 1978, *J. chem. Phys.*, **68**, 303.
- [21] SEBASTIÃO, P. J., GODINHO, M. H., RIBEIRO, A. C., GUILLON, D., and VILFAN, M., 1992, *Liq. Crystals*, **11**, 621.
- [22] ABRAGAM, A., 1961, *The Principles of Nuclear Magnetism* (Clarendon Press), Chap. VIII.
- [23] FREED, J. H., 1977, *J. chem. Phys.*, **66**, 4183.
- [24] SEBASTIÃO, P. J., RIBEIRO, A. C., NGUYEN, H. T., and NOACK, F. (to be published).
- [25] VILFAN, M., KOGOJ, M., and BLINC, R., 1987, *J. chem. Phys.*, **86**, 105.
- [26] SCHWEIKERT, K. H., and NOACK, F., 1989, *Z. Naturf. (a)*, **44**, 597.
- [27] MAZENKO, G. F., RAMASWAMY, S., and TONER, J., 1983, *Phys. Rev. A*, **28**, 1618.
- [28] TORREY, H. C., 1953, *Phys. Rev.*, **92**, 962.
- [29] VILFAN, M., and ZUMER, S., 1980, *Phys. Rev. A*, **21**, 672.
- [30] NORDIO, P. L., and BUSOLIN, P., 1971, *J. chem. Phys.*, **55**, 5485.
- [31] WOESSNER, D. E., 1962, *J. chem. Phys.*, **36**, 1; 1962, *ibid.*, **37**, 647.
- [32] VOLD, R. R., and VOLD, R. L., 1988, *J. chem. Phys.*, **88**, 1443.
- [33] KRÜGER, G. J., 1982, *Phys. Rep.*, **82**, 229.
- [34] UKLEJA, P., PIRS, J., and DOANE, J. W., 1976, *Phys. Rev. A*, **14**, 414.